MOLECULAR AND CELLULAR BIOLOGY, Oct. 1995, p. 5434–5443 Vol. 15, No. 10
0270-7306/95/$04.00+0
Copyright © 1995, American Society for Microbiology

Meis1, a *PBX1*-Related Homeobox Gene Involved in Myeloid Leukemia in BXH-2 Mice

JOHN J. MOSKOW,[1] FLORENCIA BULLRICH,[1] KAY HUEBNER,[1] IRA O. DAAR,[2] AND ARTHUR M. BUCHBERG[1]*

Jefferson Cancer Center, Jefferson Medical College, Philadelphia, Pennsylvania 19107,[1] and Laboratory of Leukocyte Biology, Biological Response Modifiers Program, National Cancer Institute-Frederick Cancer Research and Development Center, Frederick, Maryland 21702[2]

Received 16 June 1995/Returned for modification 11 July 1995/Accepted 14 July 1995

Leukemia results from the accumulation of multiple genetic alterations that disrupt the control mechanisms of normal growth and differentiation. The use of inbred mouse strains that develop leukemia has greatly facilitated the identification of genes that contribute to the neoplastic transformation of hematopoietic cells. BXH-2 mice develop myeloid leukemia as a result of the expression of an ecotropic murine leukemia virus that acts as an insertional mutagen to alter the expression of cellular proto-oncogenes. We report the isolation of a new locus, *Meis1*, that serves as a site of viral integration in 15% of the tumors arising in BXH-2 mice. *Meis1* was mapped to a distinct location on proximal mouse chromosome 11, suggesting that it represents a novel locus. Analysis of somatic cell hybrids segregating human chromosomes allowed localization of *MEIS1* to human chromosome 2p23-p12, in a region known to contain translocations found in human leukemias. Northern (RNA) blot analysis demonstrated that a *Meis1* probe detected a 3.8-kb mRNA present in all BXH-2 tumors, whereas tumors containing integrations at the *Meis1* locus expressed an additional truncated transcript. A *Meis1* cDNA clone that encoded a novel member of the homeobox gene family was identified. The homeodomain of *Meis1* is most closely related to those of the *PBX*/*exd* family of homeobox protein-encoding genes, suggesting that *Meis1* functions in a similar fashion by cooperative binding to a distinct subset of HOX proteins. Collectively, these results indicate that altered expression of the homeobox gene *Meis1* may be one of the events that lead to tumor formation in BXH-2 mice.

Chronic retroviral infections induce neoplastic disease after a long latency period (4). These retroviruses cause leukemia through either insertional activation of cellular proto-oncogenes or insertional inactivation of tumor suppressor genes (47, 54). A requisite part of the life cycle of the retrovirus is the relatively random insertion of its reverse-transcribed genome into the host genomic DNA (54). When a virus integrates near a cellular proto-oncogene, regulatory control elements present within the viral long terminal repeat (LTR) can usurp control of the proto-oncogene. The aberrant expression of the proto-oncogene results in a growth advantage for that infected cell. Additional transforming events which may or may not be due to additional integration events occur within that altered population, giving rise to a lymphoma or leukemia. Thus, some of the genes involved in the transforming events are "tagged" by the somatically acquired proviruses. Since viral integrations can occur virtually anywhere in the genome, identification of a common site of viral integration facilitates the isolation of proto-oncogenes or tumor suppressor genes involved in leukemic cell development.

A common site of viral integration is defined as a locus in which viral integrations are detected in independently derived tumors and thus represents an important event in the leukemogenic process. Genes that are located at common sites of viral integration may also be involved in neoplastic disease in humans, as in the case of *Evi1*, making murine systems an important tool for identifying genes involved in the formation of human neoplastic disease (40).

* Corresponding author. Mailing address: Jefferson Cancer Center, Jefferson Medical College, 233 S. 10th St., Room 709 BLSB, Philadelphia, PA 19107. Phone: (215) 955-4533. Fax: (215) 923-4153. Electronic mail address: Buchberg@hendrix.jci.tju.edu.

Cloning and characterization of common sites of viral integration have indicated that the integration sites are specific with respect to the type of tumor induced. Integration sites involved in T-cell and B-cell lymphomas have been well characterized (42). In addition, by using a recombinant inbred series between AKR/J and DBA/2J mice, integrations involved in B-cell lymphomas are beginning to be characterized (25). The recombinant inbred strain BXH-2 has been invaluable for the identification of proto-oncogenes involved in myeloid leukemogenesis (5). The BXH-2 recombinant inbred strain was derived from two strains of mice, C57BL/6J and C3H/HeJ (2). Although the two parental strains have a low incidence of spontaneous leukemia, nearly 100% of BXH-2 mice develop a granulocytic leukemia by 1 year of age (1, 2). This high incidence of myeloid leukemia is causally associated with high levels of ecotropic murine leukemia virus expression, beginning during embryogenesis (23). BXH-2 mice contain within their genome two defective ecotropic proviruses, *Emv1* and *Emv2* (1). Southern blot analysis of myeloid tumors, using an ecotropic virus-specific probe, reveals the presence of somatically acquired proviral integration sites in addition to the germ line *Emv1* and *Emv2* loci (5). Myeloid tumors derived from the BXH-2 mice are monoclonal in origin, as judged from the pattern of somatically acquired proviral integrations. These results are consistent with the BXH-2 ecotropic virus acting as an insertional mutagen to alter the expression of cellular proto-oncogenes or tumor suppressor genes.

Southern blot analysis using probes representing 12 different cellular proto-oncogenes revealed that of the known oncogenes tested, the c-*myb* locus exhibited proviral insertions in only 3% of the tumors (7). To identify other cellular loci involved in BXH-2 myeloid leukemogenesis, proviral integration sites were cloned and characterized. One such site, *Evi2*,

was a common site of proviral integration in 15% of the BXH-2 myeloid tumors (5). Analysis of *Evi2* revealed a complex locus encoding three small genes, *Evi2a*, *Evi2b*, and *Omgp*, located within intron 27b of the neurofibromatosis type 1 (*Nf1*) gene (33). The identification of *Evi2* provided evidence that novel, previously unidentified proto-oncogenes or tumor suppressor genes are involved in contributing to myeloid leukemia in BXH-2 mice. However, a large fraction of BXH-2 myeloid tumors contain somatically acquired proviral integrations for which the proto-oncogene involved has not yet been identified. To determine whether other proviral integration sites also identify novel cellular loci involved in myeloid leukemia, we have cloned and characterized a new proviral integration site from a BXH-2 myeloid tumor.

In this report, we present the cloning and characterization of a novel common site of viral integration in BXH-2 tumors termed *Meis1* (myeloid ecotropic viral integration site 1). Viral integrations at the *Meis1* locus were detected in 15% of the BXH-2 myeloid tumors and were localized to two clusters. The *Meis1* locus was mapped to the proximal region of mouse chromosome 11, to a position distinct from any known proto-oncogenes. The human homolog of *Meis1* maps to human chromosome 2p23-p12 near loci involved in human leukemia. A 3.8-kb transcript is detected by Northern (RNA) blot analysis of BXH-2 tumors, using probes derived from the region between two clusters of viral integrations. Cloning and sequence analysis of the gene representing the 3.8-kb transcript identified a novel member of the homeobox-containing family of transcription factors. Viral integrations within the *Meis1* locus result in a truncated *Meis1* transcript. These results indicate that *Meis1* is a novel locus involved in murine myeloid leukemia.

MATERIALS AND METHODS

Mice. The BXH-2 recombinant inbred strain was derived by Benjamin A Taylor (The Jackson Laboratory, Bar Harbor, Maine). The mice were aged by Neal G. Copeland and Nancy A. Jenkins (National Cancer Institute-Frederick Cancer Research and Development Center, Frederick, Md.). The interspecific backcross (AEJ/Gn-*a bp^H*/*a bp^H* × *Mus spretus*)F_1 × AEJ/Gn-*a bp^H*/*a bp^H* has been previously described (37).

Probes. The pECO probe is a 400-bp *Sma*I fragment isolated from the *env* gene of pAKV623 (11). The *Meis1* unique-sequence probe, P337-1, a 890-bp *Pst*I fragment, was identified from the BXH-2 genomic clone, λ337 (see below). The following unique-sequence probes were isolated from the C57BL/6J genomic lambda clones: PB6-1, a 1.2-kb *Hin*dIII-*Eco*RI fragment from λB6-G1; and PB6-2, a 700-bp *Eco*RV-*Hin*dIII fragment isolated from λB6-G2. P18-26, P19-24, and P5-23 were PCR probes generated from the spleen cDNA clone C-21 (see below). All oligomers were synthesized on an Applied Biosystems model 394 DNA synthesizer. P18-26 was generated by using oligonucleotides 5′CACTGCT GTCTTGGTGGAAC3′ and 5′CAGTGCTAAGAGAGGGAAG3′. P19-24 was generated by using oligonucleotides 5′GGTTACATGTAGTGCCACTG3′ and 5′CATGATAGACCAGTCCAACC3′. PCR conditions were as previously described (36). The thermocycler protocol was an initial denaturation step of 94°C for 4 min, followed by 30 cycles of 94°C for 30 s, 60°C for 30 s, and 72°C for 30 s.

P5-23 was a single-stranded probe representing the antisense strand of the 5′ end of the *Meis1* gene. It was generated by using the following asymmetric PCR conditions: 20 μM each dGTP, dATP, and dTTP, 50 μCi of [α-^{32}P]dCTP, 100 ng of oligomer 5′CTGTCTGATTTGGATCCTCC3′, 200 ng of *Eco*RI-digested C-21 plasmid, 0.1 U of *Taq* polymerase, and 1× PCR buffer (Boehringer Mannheim, Indianapolis, Ind.). The thermocycler protocol was an initial denaturation step of 94°C for 4 min, followed by 30 cycles of 94°C for 15 s, 55°C for 2 min, and 72°C for 2 min.

DNA isolation and Southern blot analysis. High-molecular-weight genomic DNA was isolated from frozen tissues as previously described (52). Bacteriophage and plasmid DNAs were purified by standard procedures (51). Restriction endonuclease digestions were performed as recommended by the supplier (Boehringer Mannheim). Agarose gel electrophoresis and Southern blot transfers, to Zetabind membranes (AMF Cuno, Meriden, Conn.), were performed by using standard procedures (51). Probes were labeled with [α-^{32}P]dCTP by random priming (Boehringer Mannheim). Hybridizations were performed at 65°C as described by Church and Gilbert (14). Washes were in 1× SSCP [0.18 M NaCl, 10 mM NaH_2PO_4, 1 mM EDTA [pH 7.7])–0.1% sodium dodecyl sulfate (SDS) through 0.2× SSCP–0.1% SDS at 65°C.

Screening of genomic libraries. A partial genomic library from BXH-2 myeloid tumor 337 DNA was generated by cleavage of high-molecular-weight genomic DNA with *Bcl*I (Boehringer Mannheim) and subsequent size fractionation by agarose gel electrophoresis. DNA between 13 and 14 kb in length was purified from gel slices, ligated into *Bam*HI-digested EMBL3 lambda DNA arms (Promega Corp., Madison, Wis.), and packaged by using the Gigapack packaging system (Stratagene, La Jolla, Calif.). A total of 3×10^5 plaques were screened for the provirus-containing fragment; one clone, λ337, was isolated. A C57BL/6J genomic library (Stratagene) was screened by using probes from the *Meis1* locus, using standard techniques (51). Two clones, λB6-G1 and λB6-G2, were identified from the *Meis1* locus.

Cloning of *Meis1* cDNA. Adult mouse (B6 × CBA)F_1 lung and C57BL/6J spleen cDNA libraries (Stratagene) were screened with probe P337-1, using standard techniques (51). Plasmid inserts were sequenced on an Applied Biosystems model 373A DNA sequencing system. Sequence analysis was performed with the software package from the Genetics Computer Group (Madison, Wis.) (15). Seven different clones were identified from the lung cDNA library, and four different clones were identified from the spleen cDNA library.

The alternative transcript of *Meis1* was initially identified in a *Xenopus laevis* cDNA clone, Xmeis1 (43). Reverse transcription (RT)-PCR was performed to determine the presence of this alternative spliced form in the mouse. The RT reaction mixture was as follows: 250 ng of total mouse spleen RNA, 100 ng of oligo(dT) 20-mer, 25 μM each dATP, dCTP, dGTP, and dTTP, 0.15 mg of bovine serum albumin per ml, 5 mM dithiothreitol, 26 U of RNasin (Promega), 1× first-strand buffer, and 400 U of Moloney murine leukemia virus reverse transcriptase (Gibco/BRL, Gaithersburg, Md.). The RNA, oligo(dT), and water were mixed, heated at 65°C for 15 min, and cooled on ice for 5 min, and then the other components were added. The RT reaction mixture was incubated at 37°C for 1 h and then diluted 10-fold with water for use in PCR. PCR conditions were as previously described (36), using oligomers 5′CATGATAGACCAGTCCAA CC3′ and 5′CCTGATTCGAGATCAGTCAC3′. The thermocycler protocol was an initial denaturation step of 94°C for 4 min, followed by 30 cycles of 94°C for 20 s, 60°C for 20 s, and 72°C for 20 s. PCR fragments were sequenced to confirm the presence of the alternative splice form.

RNA isolation and Northern (RNA) blot analysis. RNA was isolated from frozen mouse tissues as previously described, using guanidinium isothiocyanate (13). Twenty micrograms of total RNA was size fractionated on 1.2% formaldehyde agarose gels. Transfers to Zetabind membranes (AMF Cuno) were performed by using standard techniques (51). The Northern blot was hybridized with a single-stranded PCR product generated from probe P5-23. Northern blot hybridization was performed at 65°C as described previously (14). Washes were in 1× SSCP–0.1% SDS through 0.2× SSCP–0.1% SDS at 65°C.

Genetic mapping by interspecific backcross analysis. To detect restriction fragment length polymorphisms useful for mapping the murine loci under study, genomic DNAs from AEJ/Gn and *M. spretus* mice were digested with 14 restriction endonucleases, and individual digests were analyzed by Southern blot hybridization using probes for *Meis1*, *Egfr*, *Rel*, and *Spnb2* loci (see Table 1) (5, 60). *Glns-ps1* and *D11Mit1* were mapped by PCR that identified simple sequence length polymorphisms (16, 35). PCRs and cycling conditions were as previously described (36).

The segregation of the *M. spretus* alleles for *Meis1*, *Glns-ps1*, *D11Mit1*, *Egfr*, *Rel*, and *Spnb2* loci was monitored in random subsets of 195 N_2 mice from the interspecific backcross. Linkage of each locus typed in the interspecific backcross was analyzed by calculating the maximum-likelihood estimates of linkage parameters as described previously (17), using the computer program Spretus Madness: Part Deux (developed by Karl Smalley, Jim Averbach, Linda D. Siracusa, and A. M. Buchberg, Jefferson Cancer Institute, Philadelphia, Pa.).

Rodent-human somatic cell hybrids. Hybrid DNAs were from previously described rodent-human cell lines (22, 27) or from the NIGMS Human Genetic Mutant Cell Repository (Coriell Institute, Camden, N.J.). A hybrid, M1S10, retaining the der 2 (2qter→2p23::5q35→5qter) was isolated after fusion of the Karpas 299 human lymphoma cell line carrying the t(2;5)(p23;q35) translocation with a murine TK fibroblast line. The M1S10 hybrid was characterized by G banding and testing for the presence of relevant markers on chromosomes 2 and 5. The normal chromosome 2 and the translocation reciprocal, the der 5, were absent from the hybrid, but the der 2 was present. The J14-2 hybrid, retaining 2p12-2pter with a break in the immunoglobulin κ locus, was derived from a Burkitt's lymphoma with a t(2;8)(p12;q24) and was previously described (22).

Nucleotide sequence accession number. The nucleotide sequence of the two alternative forms of *Meis1* has been submitted to GenBank/EMBL and assigned accession numbers U33629 and U33630.

RESULTS

Identification of tumors containing common sites of viral integration. BXH-2 mice represent a unique model system for the identification of genes involved in myeloid leukemia. To date, we have identified two loci that are common sites of viral integration in BXH-2 myeloid tumors: c-*myb* and *Evi2* (5, 7). c-*myb* and *Evi2* were rearranged in 3 and 15% of the tumors

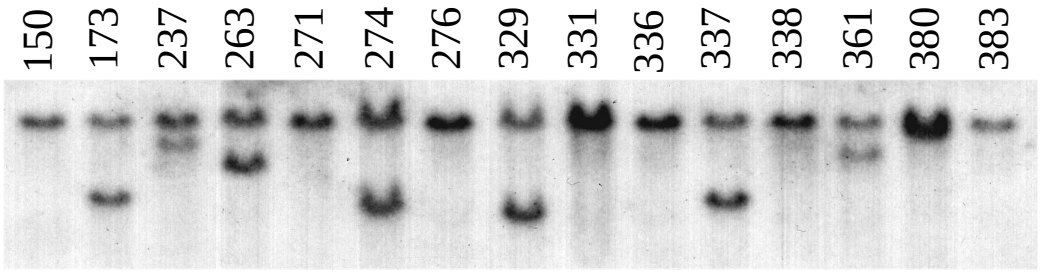

FIG. 1. Identification of a common site of viral integration in BXH-2 myeloid tumors. High-molecular-weight genomic DNAs were isolated from 16 tumor-bearing tissues of BXH-2 mice. The DNAs (5 μg per lane) were digested with *Eco*RV and analyzed by Southern blot hybridization using P337-1. The number assigned each independently derived tumor is listed above each lane. Tumors with viral integrations at the *Meis1* locus are detected by the presence of a smaller, virally rearranged restriction fragment in addition to the endogenous unrearranged fragment (29 kb). Tumors with integrations at the *Meis1* locus in cluster A are 173, 237, 263, 274, 329, 337, 361, and 380. Tumors with integrations at the *Meis1* locus in cluster B are 271, 276, and 336. Tumors which do not have integrations within the *Meis1* locus are 150, 331, 338, and 383.

examined, respectively; thus, the etiology of leukemogenesis in ~82% of the tumors was still unknown. To determine how many loci are involved in contributing to myeloid leukemia in BXH-2 mice, we sought to identify additional common sites of viral integration.

The first step in cloning new tumor-specific proviruses was to define a subclass of tumors that contain similar-size tumor-specific proviruses, suggestive of a common site of viral integration. Southern blot analysis of tumor DNAs digested with *Eco*RI and *Bcl*I, which do not cleave within the ecotropic proviral genome, and *Sac*I and *Pvu*II, which do cleave within the ecotropic proviral genome, was performed with an ecotropic virus-specific *env* probe (pECO) (11). From this analysis, we identified a restriction fragment of approximately 13.5 kb present in 13 of 65 tumors, which was suggestive of a common site of viral integration (data not shown).

Cloning of a proviral integration site from BXH-2 tumors. Southern blot analysis of *Bcl*I-digested genomic DNA from BXH-2 tumor 337 identified the 13.5-kb proviral restriction fragment in addition to two other somatically acquired proviruses. We prepared a genomic DNA library from BXH-2 tumor 337 and isolated a single clone, λ337, containing the 13.5-kb *Bcl*I restriction fragment. Restriction endonuclease analysis of λ337 revealed that it contained an 8.8-kb wild-type ecotropic provirus (20) along with 3.5 and 0.8 kb of host DNA at the 5′ and 3′ ends of the provirus, respectively. The 3.5-kb host genomic DNA fragment was subcloned and analyzed for unique-sequence fragments. The unique-sequence clone P337-1 was identified.

Identification of a common site of viral integration. BXH-2 tumors were analyzed for virally induced rearrangements by using P337-1. Southern blot analysis of genomic DNA digested with *Eco*RV and hybridized with P337-1 identified a restriction fragment of ~29 kb, representing the largest genomic region scanned by this probe. Analysis of 87 independently derived BXH-2 tumors revealed seven tumors that contained tumor-specific rearrangements at this locus (Fig. 1). The confirmation that the cloned genomic region represented a common site of viral integration in independently derived tumors indicated that there was a gene (or genes) in the region that contributed to myeloid tumorigenesis. Hence, we named the locus *Meis1*, for myeloid ecotropic viral integration site 1. Southern blot analysis of the tumor DNAs digested with *Xba*I revealed an additional tumor that contained a tumor-specific rearrangement within the *Meis1* locus. Overall, 8 of 87 tumors (9.2%) contained a rearrangement at *Meis1*. Restriction digestion of the eight tumors with *Bcl*I, *Eco*RV, *Eco*RI, *Sac*I, or *Xba*I allowed us to determine that the tumor-specific rearrangements were most likely due to the integration of wild-type ecotropic proviruses, with the exception of tumors 329 and 237 (see below) (20). The approximate location of each of the integrated proviruses was established from this analysis (Fig. 2, cluster A). In addition, we unambiguously determined the orientations of five of the eight proviral integrations. These five

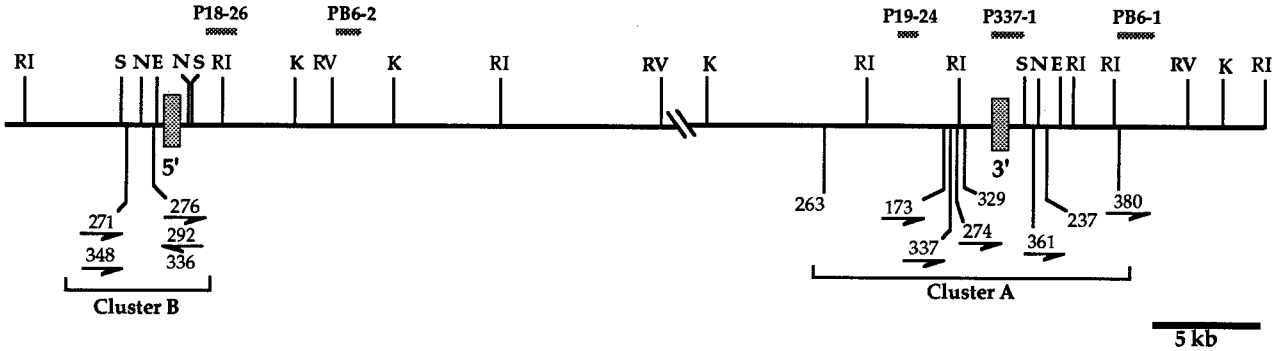

FIG. 2. Restriction map of the *Meis1* locus. The black horizontal line represents the genomic region of the *Meis1* locus in BXH-2 mice. Probes used to construct the restriction map of the locus are shown above the restriction map and are represented by the stippled lines. Probes P18-26 and P19-24 were derived from the *Meis1* cDNA. Probes PB6-1, PB6-2, and P337-1 were derived from lambda clones of genomic DNA. The approximate locations of the proviral integrations are shown by the tumor numbers below the restriction map. The orientations of the proviral integrations are shown (when known) by the arrows below the tumor numbers. The proviral integrations are clustering within two distinct regions represented by cluster A and cluster B. The stippled boxes represent the 5′ and 3′ boundaries of the *Meis1* cDNA clone. ⧹ represents the uncharacterized region of the locus. Abbreviations for restriction endonucleases: E, *Eag*I; K, *Kpn*I, N, *Nar*I; RI, *Eco*RI; RV, *Eco*RV; S, *Sac*II.

TABLE 1. Probes and RFLPs used for mapping

Locus	Probe or primers	Gene name	Enzyme	Size (kb)		Reference
				AEJ/Gn	*M. spretus*[a]	
Egfr	pHER-A64-1	Epidermal growth factor receptor gene, formerly avian erythroblastosis oncogene B (*Erbb*)	*Bcl*I	7.1	9.6	7
Rel	pBSREL	Reticuloendotheliosis oncogene	*Eco*RV	7.9	5.6	7
Spnb2	β12-1	β-Spectrin-2, nonerythrocytic	*Pst*I	6.8, 2.0, 1.7	5.8, 2.0, 1.7	54
Meis1	P337-1	Myeloid ecotropic viral integration site 1	*Hin*dIII	8.1	11.2	
D11Mit1	GGGTCTCTGAAGGCTTTGTG TGAATACAGAAGCCACGGTG	DNA segment, Chr11, MIT-1	—[b]	0.153	0.126	18
Glns-ps1	AGCTTTGGAGACAACATTAGATC TGTTCATCAGCTGAGGAATGGATG	Glutamine synthetase pseudogene 1	—	0.184	0.190	31

[a] The underlined restriction fragments identify the segregating *M. spretus* alleles monitored in the N_2 progeny.
[b] —, typed by PCR.

proviruses (173, 274, 337, 361, and 380) have the same transcriptional orientation (Fig. 2).

Restriction analysis of tumors 329 and 237 revealed that these rearrangements were most likely due to integration of deleted proviruses. Smaller restriction fragments are generated when the tumor DNA is digested with *Eco*RV and *Kpn*I, consistent with the presence of ecotropic LTR sequences; however, restriction with *Eco*RI revealed that these insertions were due to a 5.8-kb provirus, in contrast to the 8.8-kb provirus observed in the other tumors.

Chromosomal localization of the *Meis1* locus in the mouse. To determine if *Meis1* represented a new locus or a previously identified proto-oncogene, we determined its chromosomal location. An interspecific backcross mapping panel was used to localize the *Meis1* locus in the mouse. An informative polymorphism was detected when the genomic DNAs were digested with *Hin*dIII (Table 1). The segregation pattern of the *M. spretus* allele of *Meis1* was then compared with patterns of known gene and microsatellite markers that scan the entire mouse genome (8). This analysis revealed that the *Meis1* gene resides on the proximal region of mouse chromosome 11. Other proto-oncogenes known to reside in this region of mouse chromosome 11, *Egfr* and *Rel*, were localized with respect to *Meis1* (Table 1). The specific location of *Meis1* was determined by minimizing the number of multiple recombinations along the length of chromosome 11 (Fig. 3A). The order of the loci and the ratios of the number of recombinants to the total number of N_2 offspring examined are as follows: centromere-*D11Mit1*-5/77-*Egfr*-4/193-(*Meis1*, *Glns-ps1*)-1/173-*Rel*-6/168-*Spnb2*-telomere. The genetic distances between loci in centimorgans (±standard error) are as follows: centromere-*D11Mit1*-6.5 ± 2.8-*Egfr*-2.1 ± 1.0-(*Meis1*, *Glns-ps1*)-0.6 ± 0.6-*Rel*-3.6 ± 1.4-*Spnb2*-telomere. No double recombinants were detected in this interval. There were no recombinants between *Meis1* and *Glns-ps1* among 168 animals, indicating that the maximum distance between the two loci is 1.5 centimorgans at the 95% confidence limit. The segregation pattern of *Meis1* was not concordant with those of the other known proto-oncogene loci, *Rel* and *Egfr*, localized to the same region. In addition, examination of the composite linkage map of mouse chromosome 11 reveals that no other known proto-oncogene, growth factor, or growth factor receptor locus maps in the same region as *Meis1* (Fig. 3B) (34). The mapping results in the mouse suggest that *Meis1* represents a novel proto-oncogene.

Mapping of the *MEIS1* locus in the human genome. Having identified a novel locus involved in murine myeloid leukemia,

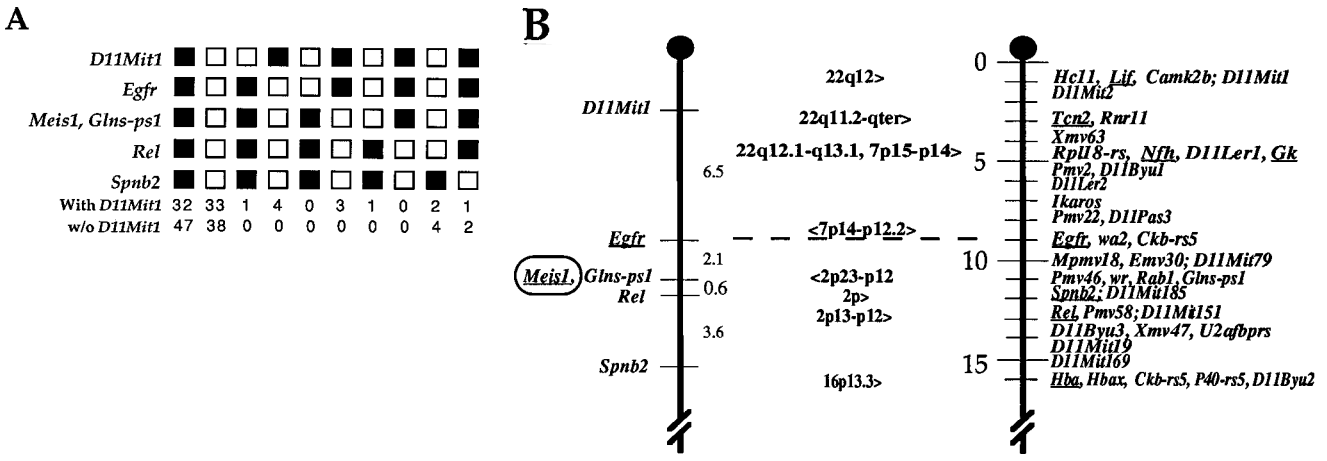

FIG. 3. Chromosomal localization of *Meis1* in the mouse. (A) Haplotype analysis of 168 N_2 progeny from the backcross. Loci monitored are listed on the left. Each column represents the chromosome identified in the N_2 offspring inherited from the (AEJ/Gn × *M. spretus*)F_1 parent. Solid squares represent the AEJ/Gn allele; open squares represent the *M. spretus* allele. The number of N_2 progeny carrying each haplotype is given at the bottom. (B) Genetic linkage map showing the location of *Meis1*. The left chromosome shows the loci typed in the backcross (Table 1), with distances between the loci given in centimorgans. The right chromosome shows a partial version of the consensus linkage map of mouse chromosome 11 (34). The two maps were arbitrarily aligned at *Egfr* (dashed line). Loci mapped in humans are underlined; gene locations on human chromosomes are shown in the middle.

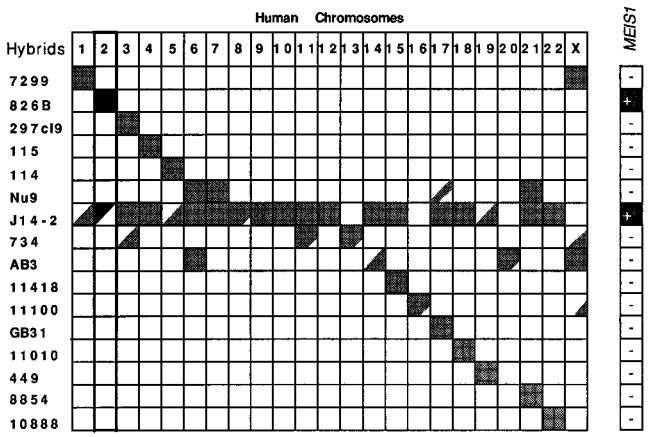

FIG. 4. Presence of the human *MEIS1* gene in a panel of 16 rodent-human somatic cell hybrids. Filled squares indicate that the hybrid named in the left column contains the chromosome indicated in the upper row. Lower right-hand diagonally filled squares indicate the presence of the long arm of the chromosome (or part of the long arm represented by a smaller fraction of stippling); upper left-hand diagonally filled squares indicate the presence of the short arm (or partial short arm) of the chromosome; open squares indicate the absence of the chromosome listed above the column. The column for chromosome 2 is boldly outlined to highlight the correlation of the presence of this chromosome (or region of the chromosome) with the presence of the *MEIS1* gene. The pattern of retention of the gene in the panel is shown at the right; presence of the locus in a hybrid is indicated by a stippled box with a plus sign, and absence of the locus is indicated by an open box enclosing a minus sign.

we wanted to determine the chromosomal location of *MEIS1* in humans. The proximal region of mouse chromosome 11 is syntenic with human chromosomes 2, 7, 16, and 22 (6, 34). To determine which human chromosome contains the human homolog of *Meis1*, we performed segregation analysis on a panel of rodent somatic cell hybrids, segregating human chromosomes. Genomic DNA isolated from the somatic cell hybrids was screened by Southern blot analysis using the evolutionarily conserved probe P337-1. The presence or absence of the human-specific restriction fragment was scored in 16 cell lines. Results indicated that *MEIS1* resided on human chromosome 2p (Fig. 4). *MEIS1* was further localized to 2p23-p12 by examining cell lines containing portions of human chromosome 2 (Fig. 5A). The interval where *MEIS1* resides on human chromosome 2 also contains several translocation breakpoints identified in B-cell leukemias (Fig. 5B) (38).

Cloning and sequence analysis of the *Meis1* gene. Having confirmed that *Meis1* is a common site of viral integration in murine myeloid tumors, we were interested in identifying the gene encoded by this locus. Southern blot analysis revealed that probe P337-1 has been conserved during evolution (data not shown), which suggests that it contains exon sequences. P337-1 was used as a probe in Northern blot analysis of RNA isolated from adult mouse tissues. Results demonstrated that P337-1 detected a 3.8-kb transcript in most tissues analyzed (data not shown). These results indicated that a gene is localized near cluster A (Fig. 2).

Adult mouse lung and spleen cDNA libraries were screened with P337-1. The largest spleen clone, C-21, was 2,860 bp long and contained an open reading frame (ORF) capable of encoding a protein of 390 amino acids (Fig. 6). C-21 also contained 434 bp of 5′ untranslated region (UTR) and 1,152 bp of 3′ UTR but did not have a polyadenylation consensus sequence. The spleen and lung sequences were overlapping, and their combination yielded a contiguous cDNA of 3,160 bp representing a near-full-length *Meis1* sequence (Fig. 6).

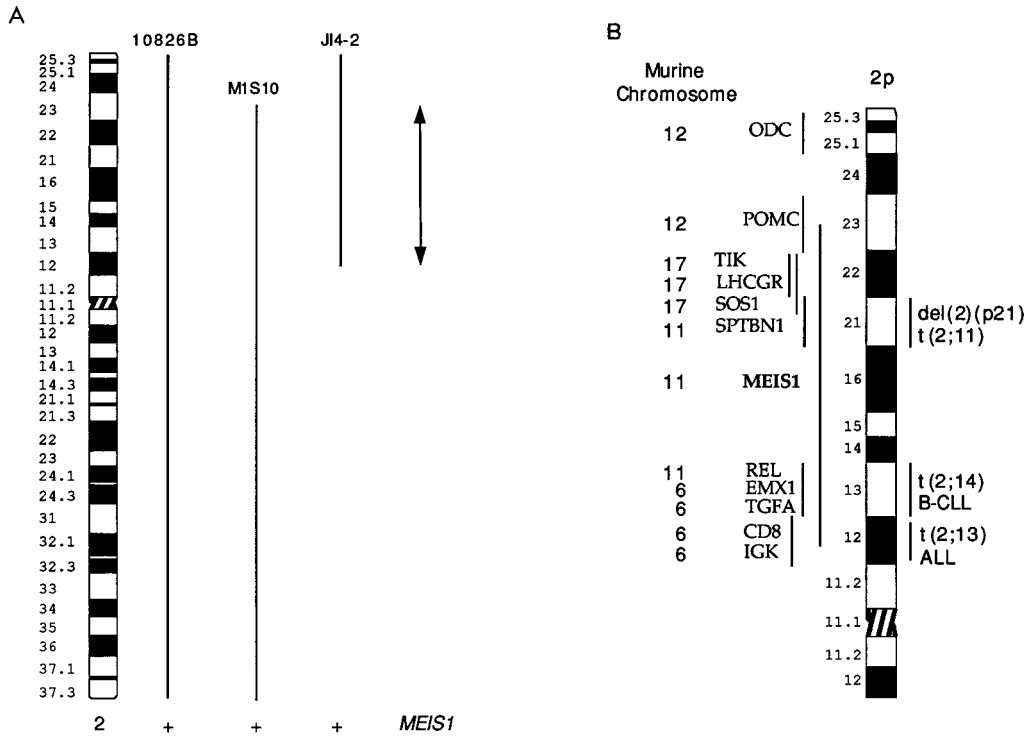

FIG. 5. Regional location of the *MEIS1* locus on the short arm of human chromosome 2. (A) The portion of chromosome 2 present in three hybrids. Each hybrid is positive for the *MEIS1* gene by Southern blot hybridization. Therefore, *MEIS1* maps to the region common to the three hybrids, the region 2p23-p12 indicated by the double-arrowheaded line. (B) Ideogram of the short arm of human chromosome 2. Map positions of *MEIS1* relative to surrounding human and murine loci are shown on the left, and those of reported neoplasia-associated chromosome aberrations are shown on the right (29, 38).

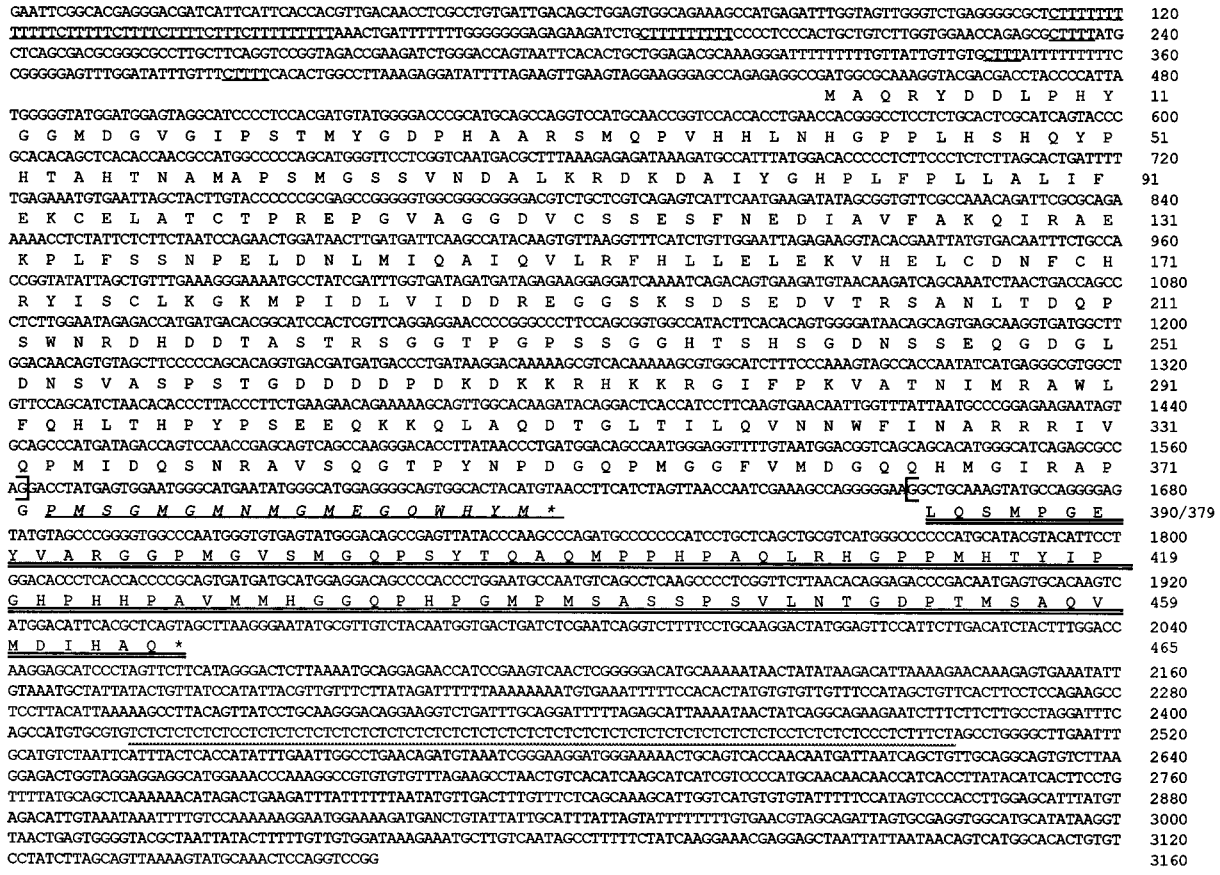

FIG. 6. Nucleotide sequence of *Meis1* cDNA and its predicted amino acid sequence. The nucleotide and amino acid sequences are numbered on the left and right. Both alternative splice forms of *Meis1* are shown. The brackets present in the nucleotide sequence represent the junction of the alternatively spliced product. The amino acids that are lost in the original transcript as a result of the alternative splice are shown in italics and underlined. The new amino acid sequence that replaces the lost region is shown by the double underline. Several $C(T)_x$ repeats are underlined in the 5′ UTR. The CT dinucleotide repeat is underlined with a dotted line in the 3′ UTR.

The nucleotide sequence and predicted ORF were used to screen for homologies in GenBank (release 88.0) and EMBL (release 39.0) databases. The only region of the *Meis1* sequence that showed homology to known genes was a 180-bp region exhibiting homology to the homeodomains of several homeobox-containing genes (31). The *Meis1* homeodomain exhibited closest homology to the homeodomains of *PBX1*, *PBX2*, *PBX3*, extradenticle (*exd*), and Knotted1 (*Kn1*) (Fig. 7) (26, 39, 46, 50, 55). This homology is limited to the homeodomain and does not extend into flanking sequences. Analysis of the *Meis1* ORF did not detect any known motifs other than the homeodomain. Analysis of the sequences of the 5′ and 3′ UTRs identified several interesting motifs. The 5′ UTR is AT rich and contains $C(T)_x$ repeats of unknown function. The 3′ UTR contains a polymorphic CT dinucleotide repeat and four ATTTA sequences which have been shown to be involved in mRNA destabilization (12).

The *Meis1* homolog of *X. laevis*, *Xmeis1*, was cloned and sequenced (43). Analysis of *Xmeis1* revealed the presence of two alternative forms, presumably a result of alternative splicing. These forms differ in the presence of a 95-nucleotide region, which results in the formation of distinct C-terminal ends of the *Xmeis1* predicted protein. Using RT-PCR, we confirmed the presence of this alternative transcript in mouse tissues. The alternative transcript is lacking 95 bp which encode the methionine-rich 18-amino-acid C-terminal end (Fig. 6). Therefore, translation of the alternative transcript results in a peptide with a novel 93-amino-acid C-terminal end due to

A

```
Meis1  KKRGIFPKVATNIMRACLFQHLTHPYPSEEQKKQLAQDTGLTILQVNNWFINARRR
PBX1   R--RN-S-Q--EVLNEYFYS--SN------A-EE--KKC-I-VS--S---G-K-I-
PBX2   R--RN-S-Q--EVLNEYFYS--SN------A-EE--KKC-I-VS--S---G-K-I-
PBX3   R--RN-S-Q--E-LNEYFYS--SN------A-EE--KKCSI-VS--S---G-K-I-
exd    R--RN-S-Q-SEVLNEYFYS--SN------A-EE--RKC-I-VS--S---G-K-I-
Kn1    --K-KL--E-RQQLLSWWD--YKW-----T--VA--ES---DLK-I------Q-K-
```

B

	Nucleotide Identity	Amino Acid Similarity	Amino Acid Identity
PBX1	52	68	50
PBX2	52	68	48
PBX3	52	68	48
exd	54	66	48
Kn1	51	68	54

FIG. 7. (A) Alignment of the *Meis1* homeodomain with *PBX1* (accession number M86546), *PBX2* (accession number X59842), *PBX3* (accession number X59841), *exd* (accession number L19295), and *Kn1* (accession number X61308) amino acid sequences. Dashes denote amino acid identity with *Meis1*; conservative substitutions are denoted with plain letters; nonconservative substitutions are given in italics. (B) The percent nucleotide identity, amino acid homology, and amino acid identity of the *Meis1* homeodomain with each of the homeodomains of the genes listed on the left.

continuation of the ORF. No known motifs were detected in this new sequence. This alternative transcript could be the result of an alternative splice site within an exon or complete loss of an exon. The latter hypothesis is most likely the case, since there is no splice acceptor site adjacent to the region of cDNA which is lost by the splice.

Identification of a second cluster of proviral integrations. The 3′ end of the *Meis1* cDNA was mapped to the middle of cluster A (Fig. 2). To determine whether viral integrations occurred at the 5′ end of the cDNA, probe p18-26, representing the 5′ end of the *Meis1* cDNA, was used to screen the 87 BXH-2 tumors. Southern blot analysis using *Eco*RV-digested genomic DNA identified five additional tumors that contained viral integrations. These proviral integrations represented a second cluster of integration sites (Fig. 2, cluster B) located more than 67 kb upstream from cluster A (data not shown). Restriction endonuclease analysis of these new tumors revealed that the integration sites were localized to a 1.6-kb region. Using a combination of restriction endonucleases, we determined the orientations of four of the five proviruses. Three of the proviruses have the same transcriptional orientation as those located in cluster A, while the fourth provirus has the opposite direction of transcription. The identification of proviral integration sites flanking the gene strongly indicates that *Meis1* is a gene that contributes to myeloid leukemia in BXH-2 mice.

Identification of CpG islands flanking the *Meis1* gene. Restriction endonuclease analysis of the viral clusters detected the presence of two CpG islands which are commonly present at the 5′ end of genes (3). We performed double digestions using methylation-sensitive *Eag*I, *Nar*I, *Sac*II, *Not*I, or *Sfi*I and methylation-insensitive *Eco*RV, *Bcl*I, or *Kpn*I. Three of the methylation-sensitive enzymes (*Eag*I, *Nar*I, *Sac*II) were determined to be present within each of these CpG islands. Surprisingly, each cluster of proviral integrations is located within one of the CpG islands. The CpG island present at cluster B (Fig. 2) is associated with the 5′ end of the *Meis1* gene, while the CpG island present at cluster A (Fig. 2) may be associated with the 5′ end of a second gene located downstream of the *Meis1* gene.

The expression of *Meis1* is altered by the proviral integrations. Having identified a transcript at the *Meis1* locus, the next step was to determine whether proviral integrations alter the expression of *Meis1*. With P337-1, Northern blot analysis of tumors with and without viral integrations at the *Meis1* locus failed to detect any differences in the 3.8-kb mRNA (data not shown). However, examination of the *Meis1* restriction map (Fig. 2) reveals that P337-1 lies in the middle of cluster A. Since P337-1 represents the 3′ end of the *Meis1* gene, a predicted result is that the viral integrations in cluster A would result in either increased expression due to viral LTR enhancer sequences or premature termination of the transcript by termination sequences present in the viral LTR (47). A consequence of the latter model would be that P337-1 would not detect any differences in transcription; therefore, we used P5-23, which represents the 5′ end of the *Meis1* gene. Results of Northern blot analysis using P5-23 revealed the presence of a second, shorter transcript in two tumors, 274 and 263 (Fig. 8). We also detected a truncated transcript in tumor 329 that is the same size as the truncated transcript detected in tumor 274 (data not shown). In addition, these same tumors have an elevated level of expression of the 3.8-kb transcript. This 3.8-kb transcript may represent upregulation of the normal *Meis1* mRNA or increased expression of an alternative *Meis1*-proviral fusion mRNA. The presence of the truncated transcript in the BXH-2 tumors correlated with viral integrations being present within cluster A of the *Meis1* locus. Tumors which did not have integrations at the *Meis1* locus and tumor 292, which has an integration within cluster B, showed low levels of *Meis1* expression. These results demonstrate that viral integrations in cluster A disrupt the expression of the *Meis1* gene.

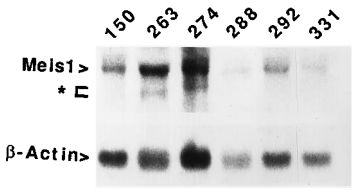

FIG. 8. Expression of *Meis1* in BXH-2 tumors. Twenty micrograms of total RNA obtained from BXH-2 liver, infiltrated with tumor, was examined by Northern blot analysis. Tumors containing an integration at the *Meis1* locus in cluster A are 274 and 263. Tumor 292 represents a tumor with a viral integration at the *Meis1* locus in cluster B. Tumors 150, 288, and 331 do not have viral integrations at the *Meis1* locus. The endogenous 3.8-kb *Meis1* transcript was detected by using a single-stranded probe representing the 5′ end of a cDNA clone present within the *Meis1* locus. Truncated bands are identified by the asterisk. β-Actin was used as a control for uniform loading of RNA.

DISCUSSION

The BXH-2 murine recombinant inbred strain provides an ideal system for the identification of genes involved in myeloid leukemia. In this report, we describe the identification and characterization of a new common site of viral integration, *Meis1*. Fifteen percent of the tumors analyzed contain proviral integrations at the *Meis1* locus. Analysis of the *Meis1* locus demonstrated that there are two clusters of integration sites (Fig. 2, clusters A and B) in a region that encodes a novel member of the homeobox gene family.

Meis1 was localized to proximal mouse chromosome 11 (Fig. 3B). The placement of *Meis1* in a region distinct from other known proto-oncogene, growth factor, and receptor loci suggested that it represented a novel gene. *Meis1* was shown to be tightly linked to the *Glns-ps1* locus. Previous reports have demonstrated that the mouse neurological mutation wobbler (*wr*) is also very tightly linked to *Glns-ps1* (57). *wr* homozygous mice exhibit a partial motor neuron degeneration, sperm defects, and overexpression of interleukin 1 by peripheral macrophages (19, 28, 30). Because of the close linkage of the two loci, *Meis1* represents a candidate gene for the *wr* mutation. Analysis of the genetic organization and expression pattern of *Meis1* in *wr* mutant mice is required to test whether *Meis1* is *wr*.

The human homolog of *Meis1* was localized to human chromosome 2, in the region 2p23-p12. The human homologs of two other genes on mouse chromosome 11, *Rel* and *Spnb2*, also reside on human chromosome 2p, and define a syntenic region between these two chromosomes. Our mapping data demonstrated that the order of these genes in the mouse is centromere-*Meis1-Rel-Spnb2*-telomere. In contrast, the order of *MEIS1*, *REL*, and *SPTBN1* in the human genome is not known. If identical gene orders for the mouse and human genomes are found, then *Meis1*, *Rel*, and *Spnb2* constitute a conserved linkage group (44). This conserved linkage group can be used to make predictions about subsequent genes localized to this region in either the mouse or human genome. Regardless of the absolute order of these genes, the somatic cell hybrid data place *MEIS1* in a region between the *IGK* (2p12) and *ALK* (2p23) loci (41). Recently, a search of the EMBL database (version 42.0) identified a random human clone, *D2S134* (accession number Z16763), which shows 80% nucleotide identity to *Meis1* and has been localized to human chromosome 2p14-

p13 (56). The high sequence identity and comparative map location suggest that *D2S134* represents the human *MEIS1* locus. Alterations in this region of human chromosome 2 have been identified in B-cell chronic lymphocytic leukemias and acute lymphocytic leukemias (29, 38). Thus, the finding that *Meis1* is a common site of viral integration in murine leukemic cells, coupled with its corresponding human map location in the vicinity of breakpoints found in B-cell chronic lymphocytic leukemias and acute lymphocytic leukemias, suggests that the *MEIS1* locus should be examined for its involvement in human leukemia.

The *Meis1* gene product is a novel member of the homeobox-containing family of transcription factors. *Meis1* is most closely related to the *PBX* family of homeobox-containing genes. The homology is limited to the homeodomains of these genes. *PBX1* was originally identified as the fusion partner of E2A in a translocation breakpoint found in human pre-B-cell leukemias (26, 46). *PBX2* and *PBX3* were identified through their homology with *PBX1* (39). The *Drosophila melanogaster* homolog of *PBX1* is *exd*, which regulates homeobox genes involved in segmental identity (50). Kn1 is a maize homeobox protein involved in leaf fate determination (55). *PBX1* and *exd* have recently been shown to modify the binding specificity of a distinct subset of HOX proteins by cooperative binding through a conserved motif (9, 10, 24, 53). Some of these interacting domains have been mapped to the homeodomain (59). The homology of *Meis1* with *PBX1* and *exd* suggests that *Meis1* performs a similar function but with respect to a different subset of homeobox-containing genes.

An alternative splice in which the C terminus of *Meis1* was altered was identified. Although there is a significant difference between the alternatively spliced forms, the homeodomain remains unchanged, suggesting that the proteins may still bind identical target sequences. Since regulators of DNA binding are known to reside adjacent to the homeodomain, it is possible that the different forms of *Meis1* differentially regulate gene expression (21).

Southern blot analysis of the *Meis1* locus has demonstrated the presence of two clusters of viral integrations that are located within or near two CpG islands. CpG islands have been implicated in the regulation of gene expression and are commonly found at the 5′ ends of genes (3). The CpG island within cluster B represents the 5′ end of the *Meis1* gene, while the CpG island within cluster A most likely represents the 5′ end of a second gene at the *Meis1* locus. Thus, viral integrations that occur at the 3′ end of *Meis1* (cluster A; Fig. 2) and the 5′ end of a neighboring gene may affect the expression of both genes, as demonstrated for the *Int2*/*Hst* gene cluster (49).

The clustering of integrations around the 5′ and 3′ ends of genes is consistent with the modes of activation of gene transcription by integrated proviruses (54). Integrations occurring within the 5′ end of *Meis1* could increase expression by promoter and enhancer sequences present within the LTR of the provirus. Integrations at the 3′ end of a gene are also able to upregulate the basal level of expression by enhancer sequences present in the viral LTR. Integrations that occur within the 3′ end of a gene could result in premature termination of the primary transcript, resulting in loss of coding sequences or 3′ UTR regulatory elements. For example, viral integrations within the 3′ end of the *Pim1* gene truncate the 3′ UTR, which contains important AU-rich motifs involved in mRNA instability (58). Also, integrations within the c-*erbB*/*Egfr* gene lead to loss of the ligand binding domain, resulting in constitutive activation of the protein (45).

To determine whether viral integrations were altering *Meis1* expression, we examined RNA from tumor-infiltrated BXH-2 liver that had tumors containing viral integrations within *Meis1* (tumors 263, 274, and 292). Normal adult liver has a low but detectable level of *Meis1* expression (data not shown). Therefore, a low background level of *Meis1* expression, in addition to the contribution from the infiltrating leukemic cells, should be observed in the tumor-containing liver samples. Quantitative comparisons of *Meis1* expression is difficult because the amount of tumor infiltrating the liver cannot be quantitated. In particular, tumor 292, which has a viral integration in the 5′ end of *Meis1* (cluster B; Fig. 2), has expression levels comparable to those of the other tumors that do not have *Meis1* integrations (Fig. 8). This result is probably due to a low level of leukemic infiltration into the liver in the 292 mouse.

Regardless of the inability to detect quantitative changes in *Meis1* expression, qualitative changes can be observed. The results of Northern blot analyses of tumors 263, 274 (Fig. 8), and 329 (data not shown) clearly demonstrate that the integration of viruses in cluster A results in a shorter *Meis1* transcript, presumably as a result of premature termination by viral LTRs. The exon sequences represented by P337-1 are most likely the 3′ end of the *Meis1* gene which is truncated by the integrated proviruses. This conclusion is supported by the fact that P337-1 fails to detect the truncated transcripts in BXH-2 tumors with integrations in *Meis1* (data not shown). In tumor 263, there may be loss of additional exon sequences located upstream of P337-1, a possibility supported by the more upstream location of the 263 integration and the shorter mRNA (Fig. 8). In addition to the truncated transcript, there also appears to be an increased level of expression of the 3.8-kb *Meis1* transcript (Fig. 8). Since P337-1 did not detect the elevated 3.8-kb transcript in these tumors, this mRNA is probably a result of a *Meis1*-provirus fusion (data not shown). It is unclear what effect truncation of the 3′ exons would have on each of the *Meis1* transcripts. Truncation of the original 390-amino-acid form would cause loss of the 3′ UTR sequences, which could lead to increased mRNA stability. Truncation of the larger alternative splice form would truncate 94 amino acids and could lead to a protein with a distinct function. It is also possible that the viral integrations in cluster A alter *Meis1* expression by causing a shift in the relative levels of the different spliced forms of *Meis1*. An aberrant mRNA homeostasis may contribute to the transformation of these hematopoietic cells. The Northern blot results provide strong evidence that the integrating proviruses are altering the normal expression and/or regulation of the *Meis1* gene.

It is well known that homeobox genes play an important role in the differentiation and proliferation of hematopoietic cells (32). Alteration of the expression of homeobox genes has been shown to be involved in the development of leukemia (18, 48). We propose that viral integrations in *Meis1* result in a dysregulation of the protein which leads to a block in differentiation or an increase in proliferation of developing myeloid cells. This alteration in the differentiation pathway leads to the formation of the myeloid leukemia.

To date, viral integrations have been identified in three loci, c-*myb*, *Evi2*, and *Meis1*, in BXH-2 myeloid tumors. These viral integrations account for only 32% of the BXH-2 tumors analyzed. In addition, no overlap in the integration sites exists in these tumors. These results indicate that in 68% of the tumors, viral integrations are occurring in other loci and that only one of the multiple genes involved in transformation has been identified for these tumors. Analysis of the remaining BXH-2 tumors for common sites of viral integration as well as the identification of cooperating oncogenes for the existing loci are crucial to complete the BXH-2 story of how and why a myeloid stem cell goes awry in tumorigenesis.

The identification of the genes involved in leukemia may provide different levels of eventual therapeutic approaches. Many inroads have been made to identify and characterize genes involved in human myeloid leukemias. Use of animal model systems greatly expands the ability to identify genes involved in leukemogenesis, some of which will be involved in human disease. However, even if these murine genes are not directly involved in human leukemia, by virtue of their being localized at translocation breakpoints, they will still enable further characterization of the pathways that result in the neoplastic transformation of myeloid cells.

ACKNOWLEDGMENTS

This work was supported by NIH grant CA58586 from the National Cancer Institute (A.M.B.), NRSA training grant 1 T32 HL07780-01 (J.J.M.), USPHS grant CA51083 (K.H.), and NRSA training grant 5 F31 CA60352-03 from National Cancer Institute (F.B.).

We thank Warren E. Zimmer (Department of Structural and Cellular Biology, University of South Alabama, Mobile) for the kind gift of the β-spectrin probe, Neal G. Copeland and Nancy A. Jenkins (ABL-Basic Research Program, NCI-Frederick Cancer Research and Development Center, Frederick, Md.) for the BXH-2 tumor samples, and Teresa Druck for technical assistance. We thank Linda D. Siracusa and Jay Rothstein and for helpful and valuable discussions and critical reading of the manuscript.

REFERENCES

1. **Bedigian, H. G., D. A. Johnson, N. A. Jenkins, N. G. Copeland, and R. Evans.** 1984. Spontaneous and induced leukemias of myeloid origin in recombinant inbred BXH mice. J. Virol. **51:**586–594.
2. **Bedigian, H. G., B. A. Taylor, and H. Meier.** 1981. Expression of murine leukemia viruses in the highly lymphomatous BXH-2 recombinant inbred mouse strain. J. Virol. **39:**632–640.
3. **Bird, A. P.** 1986. CpG-rich islands and the function of DNA methylation. Nature (London) **321:**209–213.
4. **Bishop, J. M.** 1987. The molecular genetics of cancer. Science **235:**305–311.
5. **Buchberg, A. M., H. G. Bedigian, N. A. Jenkins, and N. G. Copeland.** 1990. *Evi-2*, a common integration site involved in murine myeloid leukemogenesis. Mol. Cell. Biol. **10:**4658–4666.
6. **Buchberg, A. M., E. Brownell, S. Nagata, N. A. Jenkins, and N. G. Copeland.** 1989. A comprehensive genetic map of murine chromosome 11 reveals extensive linkage conservation between mouse and human. Genetics **122:** 153–161.
7. **Buchberg, A. M., N. A. Jenkins, and N. G. Copeland.** Unpublished data.
8. **Buchberg, A. M., and L. D. Siracusa.** Unpublished data.
9. **Chan, S.-K., L. Jaffe, M. Capovilla, J. Botas, and R. S. Mann.** 1994. The DNA binding specificity of ultrabithorax is modulated by cooperative interactions with extradenticle, another homeoprotein. Cell **78:**603–615.
10. **Chang, C.-P., W.-F. Shen, S. Rozenfeld, H. J. Lawrence, C. Largman, and M. L. Cleary.** 1995. Pbx proteins display hexapeptide-dependent cooperative DNA binding with a subset of Hox proteins. Genes Dev. **9:**663–674.
11. **Chattopadhyay, S. K., M. R. Lander, E. Rands, and D. R. Lowy.** 1980. Structure of endogenous murine leukemia virus DNA in mouse genomes. Proc. Natl. Acad. Sci. USA **77:**5774–5778.
12. **Chen, C.-Y. A., T.-M. Chen, and A.-B. Shyu.** 1994. Interplay of two functionally and structurally distinct domains of the c-*fos* AU-rich element specifies its mRNA-destabilizing function. Mol. Cell. Biol. **14:**416–426.
13. **Chomczynski, P., and N. Sacchi.** 1987. Single-step method of RNA isolation by acid guanidium thiocyanoate-phenol-chloroform extraction. Anal. Biochem. **162:**156–159.
14. **Church, G. M., and W. Gilbert.** 1984. Genomic sequencing. Proc. Natl. Acad. Sci. USA **81:**1991–1995.
15. **Devereux, J., P. Haeberli, and O. Smithies.** 1984. A comprehensive set of sequence analysis programs for the VAX. Nucleic Acids Res. **12:**387–395.
16. **Dietrich, W., H. Katz, S. E. Lincoln, H. S. Shin, J. Friedman, N. C. Dracopoli, and E. S. Lander.** 1992. A genetic map of the mouse suitable for typing intraspecific crosses. Genetics **131:**423–447.
17. **Green, M. C.** 1981. Gene mapping, p. 105–117. *In* H. L. Foster, J. D. Smith, and J. G. Fox (ed.), The mouse in biomedical research. Academic Press, New York.
18. **Hatano, M., C. W. M. Roberts, M. Minden, W. M. Crist, and S. J. Korsmeyer.** 1991. Deregulation of a homeobox gene, HOX11, by the t(10;14) in T cell leukemia. Science **253:**79–82.
19. **Heimann, P., S. Laage, and H. Jockusch.** 1991. Defect of sperm assembly in a neurological mutant of the mouse, wobbler (*wr*). Differentiation **47:**77–83.
20. **Herr, W.** 1984. Nucleotide sequence of AKV murine leukemia virus. J. Virol. **49:**471–478.
21. **Hoey, T., R. Warrior, J. Manak, and M. Levine.** 1988. DNA-binding activities of the *Drosophila melanogaster* even skipped protein are mediated by its homeo domain and influenced by protein context. Mol. Cell. Biol. **8:**4598–4607.
22. **Huebner, K., T. Druck, C. M. Croce, and H.-J. Thiesen.** 1991. Twenty-seven nonoverlapping zinc finger cDNAs from human T cells map to nine different chromosomes with apparent clustering. Am. J. Hum. Genet. **48:**726–740.
23. **Jenkins, N. A., N. G. Copeland, B. A. Taylor, H. G. Bedigian, and B. K. Lee.** 1982. Ecotropic murine leukemia virus DNA content of normal and lymphomatous tissues of BXH-2 recombinant inbred mice. J. Virol. **42:**379–388.
24. **Johnson, F. B., E. Parker, and M. A. Krasnow.** 1995. Extradenticle protein is a selective cofactor for the Drosophila homeotics: role of the homeodomain and YPWM amino acid motif in the interaction. Proc. Natl. Acad. Sci. USA **92:**739–743.
25. **Justice, M. J., H. C. Morse III, N. A. Jenkins, and N. G. Copeland.** 1994. Identification of Evi-3, a novel common site of retroviral integration in mouse AKXD B-cell lymphomas. J. Virol. **68:**1293–1300.
26. **Kamps, M. P., C. Murre, X.-H. Sun, and D. Baltimore.** 1990. A new homeobox gene contributes the DNA binding domain of the t(1;19) translocation protein in pre-B ALL. Cell **60:**547–555.
27. **Kastury, K., T. Druck, K. Huebner, C. Barletta, D. Acampora, A. Simeone, A. Faiella, and E. Boncinelli.** 1994. Chromosome locations of human *EMX* and *OTX* genes. Genomics **22:**41–45.
28. **Kaupmann, K., D. Simon-Chazottes, J.-L. Guènet, and H. Jockusch.** 1992. Wobbler, a mutation affecting motoneuron survival and gonadal functions in the mouse, maps to proximal chromosome 11. Genomics **13:**39–43.
29. **Kees, U. R., L. J. Campbell, J. Ford, M. L. N. Willoughby, S. E. Peroni, P. R. Ranford, and O. M. Garson.** 1995. New translocation t(2;13)(p12;q34) and rearrangement of the MLL gene in a childhood leukemia cell line. Genes Chromosomes Cancer **12:**201–208.
30. **Kopmels, B., E. E. Wollman, J. M. Guastavino, N. Delhaye-Bouchaud, D. Fradelizi, and J. Mariani.** 1990. Interleukin-1 hyperproduction by in vitro activated peripheral macrophages from cerebellar mutant mice. J. Neurochem. **55:**1980–1985.
31. **Kornberg, T. B.** 1993. Understanding the homeodomain. J. Biol. Chem. **268:**26813–26816.
32. **Lawrence, H. J., and C. Largman.** 1992. Homeobox genes in normal hematopoiesis and leukemia. Blood **80:**2445–2453.
33. **Li, Y., P. O'Connell, H. H. Breidenbach, R. Cawthon, J. Stevens, G. Xu, S. Neil, M. Robertson, R. White, and D. Viskochil.** 1995. Genomic organization of the neurofibromatosis 1 Gene. Genomics **25:**9–18.
34. **Lossie, A. C., M. MacPhee, A. M. Buchberg, and S. A. Camper.** 1994. Mouse chromosome 11. Mamm. Genome **5:**S164–S180.
35. **Love, J. M., A. M. Knight, M. A. McAleer, and J. A. Todd.** 1990. Towards construction of a high resolution map of the mouse genome using PCR-analysed microsatellites. Nucleic Acids Res. **18:**4123–4130.
36. **Ma, Q., H. Alder, K. K. Nelson, D. Chatterjee, Y. Gu, T. Nakamura, E. Canaani, C. M. Croce, L. D. Siracusa, and A. M. Buchberg.** 1993. Analysis of the murine *All-1* gene reveals conserved domains with human *ALL-1* and identifies a motif shared with DNA methyltransferases. Proc. Natl. Acad. Sci. USA **90:**6350–6354.
37. **Marini, J. C., K. K. Nelson, J. Battey, and L. D. Siracusa.** 1993. The pituitary hormones arginine vasopressin-neurophysin II and oxytocin-neurophysin I show close linkage with interleukin-1 on mouse chromosome 2. Genomics **15:**200–202.
38. **Mitelman, F., Y. Kaneko, and J. Trent.** 1991. Report of the committee on chromosome changes in neoplasia. Cytogenet. Cell Genet. **58:**1053–1079.
39. **Monica, K., N. Galili, J. Nourse, D. Saltman, and M. L. Cleary.** 1991. *PBX2* and *PBX3*, new homeobox genes with extensive homology to the human proto-oncogene *PBX1*. Mol. Cell. Biol. **11:**6149–6157.
40. **Morishita, K., E. Parganas, C. L. William, M. H. Whittaker, H. Drabkin, J. Oval, R. Taetle, M. B. Valentine, and J. N. Ihle.** 1992. Activation of *EVI1* gene expression in human acute myelogenous leukemias by translocations spanning 300-400 kilobases on chromosome band 3q26. Proc. Natl. Acad. Sci. USA **89:**3937–3941.
41. **Morris, S. W., M. N. Kirstein, M. B. Valentine, K. G. Dittmer, D. N. Shapiro, D. L. Saltman, and A. T. Look.** 1994. Fusion of a kinase gene, *ALK*, to a nucleolar protein gene, *NPM*, in non-Hodgkin's lymphoma. Science **263:** 1281–1284.
42. **Mucenski, M. L., D. J. Gilbert, B. A. Taylor, N. A. Jenkins, and N. G. Copeland.** 1987. Common sites of viral integration in lymphomas arising in AKXD recombinant inbred mouse strains. Oncogene Res. **2:**33–48.
43. **Muzenski, K., J. J. Moskow, A. M. Buchberg, and I. O. Daar.** Unpublished results.
44. **Nadeau, J. H.** 1989. Maps of linkage and synteny homologies between mouse and man. Trends Genet. **5:**82–86.
45. **Nilsen, T. W., P. A. Maroney, R. G. Goodwin, F. M. Rottman, L. B. Crittenden, M. A. Raines, and H. J. Kung.** 1985. *c-erbB* activation in ALV-induced erythroblastosis: novel RNA processing and promoter insertion result in expression of an amino-truncated EGF receptor. Cell **41:**719–726.
46. **Nourse, J., J. D. Mellentin, N. Galili, J. Wilkinson, E. Stanbridge, S. D.**

Smith, and M. L. Cleary. 1990. Chromosomal translocation t(1;19) results in synthesis of a homeobox fusion mRNA that codes for a potential chimeric transcription factor. Cell **60:**535–545.
47. **Nusse, R.** 1986. The activation of cellular oncogenes by retroviral insertion. Trends Genet. **2:**244–247.
48. **Perkins, A., K. Kongsuwan, J. Visvader, J. M. Adams, and S. Cory.** 1990. Homeobox gene expression plus autocrine growth factor production elicits myeloid leukemia. Proc. Natl. Acad. Sci. USA **87:**8398–8402.
49. **Peters, G., S. Brookes, R. Smith, M. Placzek, and C. Dickson.** 1989. The mouse homolog of the *hst/k-FGF* gene is adjacent to *int-2* and is activated by proviral insertion in some virally induced mammary tumors. Proc. Natl. Acad. Sci. USA **86:**5678–5682.
50. **Rauskolb, C., M. Peifer, and E. Wieschaus.** 1993. *extradenticle*, a regulator of homeotic gene activity, is a homolog of the homeobox-containing human proto-oncogene PBX1. Cell **74:**1101–1112.
51. **Sambrook, J., E. F. Fritsch, and T. Maniatis.** 1989. Molecular cloning: a laboratory manual. Cold Spring Harbor Laboratory Press, Cold Spring Harbor, N.Y.
52. **Siracusa, L. D., A. M. Buchberg, N. G. Copeland, and N. A. Jenkins.** 1989. Recombinant inbred strain and interspecific backcross analysis of molecular markers flanking the murine agouti coat color locus. Genetics **122:**669–679.
53. **Van Dijk, M. A., and C. Murre.** 1994. Extradenticle raises the DNA binding specificity of homeotic selector gene products. Cell **78:**617–624.
54. **Van Lohuizen, M., and A. Berns.** 1990. Tumorigenesis by slow-transforming retroviruses—an update. Biochim. Biophys. Acta **1032:**213–235.
55. **Vollbrecht, E., B. Veit, N. Sinha, and S. Hake.** 1991. The developmental gene *knotted-1* is a member of a maize homeobox gene family. Nature (London) **350:**241–243.
56. **Weissenbach, J., G. Gyapay, C. Dib, A. Vignal, J. Morissette, P. Millasseau, G. Vaysseix, and M. Lathrop.** 1992. A second-generation linkage map of the human genome. Nature (London) **359:**794–801.
57. **Wichmann, H., H. Jockusch, J.-L. Guenet, D. Gallwitz, and K. Kaupmann.** 1992. The mouse homolog to the ras-related yeast gene *YPT1* maps on chromosome 11 close to the wobbler (*wr*) locus. Mamm. Genome **3:**467–468.
58. **Wingett, D., R. Reeves, and N. S. Magnuson.** 1992. Characterization of the testes-specific *pim-1* transcript in rat. Nucleic Acids Res. **20:**3183–3189.
59. **Zappavigna, V., D. Sartori, and F. Mavilio.** 1994. Specificity of HOX protein function depends on DNA-protein and protein-protein interaction, both mediated by the homeo domain. Genes Dev. **8:**732–744.
60. **Zimmer, W. E., Y. P. Ma, and S. R. Goodman.** 1991. Identification of a mouse brain beta-spectrin cDNA and distribution of its mRNA in adult tissues. Brain Res. Bull. **27:**187–193.